

Study of Dynamic Sorption in Adsorption Refrigeration Cycle

Adil A. Al-Hemiri

Professor

Eng. College

Baghdad University

E-mail : adilawad2001@yahoo.com

Mohammed A. Atiya

Assistant Professor

Research & Development Department

Ministry of Higher Education & S.R.

E-mail : mohatiya1965@gmail.com

Farkad A. Lattieff

Assistant instructor

Research & Development Department

Ministry of Higher Education & S.R.

E-mail : farkad400@yahoo.com

ABSTRACT

This paper shows the characteristics of temperature and adsorbed (water vapor) mass rate distribution in the adsorber unit which is the key part to any adsorption refrigeration system. The temperature profiles of adsorption/desorption phases (Dynamic Sorption) are measured experimentally under the operating conditions of 90°C hot water temperature, 30°C cooling water temperature, 35°C adsorption temperature and cycle time of 40 min. Based on the temperature profiles, The mass transfer equations for the annulus adsorbent bed are solved to obtain the distribution of adsorption velocity and adsorbate concentration using non-equilibrium model. The relation between the adsorption velocity with time is investigated during the process of adsorption. The practical cycles of adsorption and desorption were stated dependent on the variables obtained from the experiment and equations calculations.

The results show that the adsorption velocity is diminished after a period of 20 min. The maximum value of the adsorbed water vapor concentration on silica gel is 0.12 kg water/kg adsorbent (adsorption phase) and the minimum value of the water content into silica gel is 0.04 kg water/kg adsorbent (desorption phase) producing a dynamic sorption of $\Delta x = 0.08$ kg water/kg adsorbent.

Key words: adsorption, refrigeration, silica gel-water, mass transfer

دراسة ديناميكية الامتزاز في دورة التبريد الامتزازية

م.م فرقد علي لطيف
دائرة البحث والتطوير
وزارة التعليم العالي والبحث العلمي

ا.م.د. محمد عبد عطية
دائرة البحث والتطوير
وزارة التعليم العالي والبحث العلمي

ا.د. عادل احمد عوض
كلية الهندسة
جامعة بغداد

الخلاصة

يعرض هذا البحث خصائص توزيع الحرارة وجريان الكتلة للمادة الممتزة (بخار الماء) في وحدة الامتزاز والتي تمثل الجزء المفتاح لأي منظومة تبريد امتزازية. إن شكل التوزيع الحراري لأطوار الامتزاز والانبعث (ديناميكية الامتصاص) تم قياسه عمليا تحت ظروف تشغيلية من درجة حرارة 90 °م للماء الساخن ودرجة حرارة 30 °م للماء البارد ودرجة حرارة 35 °م للامتزاز وزمن دورة 40 دقيقة. اعتمادا على شكل التوزيع الحراري فإن معادلات انتقال المادة لحشوة الحبيبات الدائرية قد حلت للحصول على توزيع سرعة الامتزاز وتركيز المادة الممتزة باستعمال موديل اللاتوازن. كذلك العلاقة بين تغير سرعة الامتزاز مع الزمن قد تم التحقق منها أثناء عملية الامتزاز. تم تحديد الدورة العملية للامتزاز والانبعث بالاعتماد على المتغيرات التي تم الحصول عليها من التجربة وحسابات المعادلات. النتائج بينت ان سرعة الامتزاز تتلاشى بعد مرور 20 دقيقة. كانت أعلى قيمة لتركيز بخار الماء الممتز في السليكا جل 0,12 كغم ماء/كغم مازة (أثناء الامتزاز) وأوطأ قيمة كانت 0,04 كغم ماء/كغم مازة في السليكا جل (أثناء الانبعث) مولدة" ديناميكية امتزاز 0,08 كغم ماء/كغم مازة.

الكلمات الرئيسية : الامتزاز, التبريد, السليكا جل-ماء, انتقال المادة

1. INTRODUCTION

Adsorption (solid–vapor) refrigeration is analogous to liquid–vapor absorption, except the refrigerant is adsorbed onto a solid desiccant (freeze dried) rather than absorbed into a liquid (dissolved) as in liquid–vapor heat pumps. The adsorption cycle **Fig. 1** proceeds as follows **Lambert, 2007**.

1. At state 1, a cool canister filled with adsorbent, an adsorber, is saturated with refrigerant at slightly below P_e . The adsorber is heated and desorbs refrigerant vapor isosterically (i.e., at constant total mass in the adsorber), pressurizing it to state 2, slightly above P_c , which opens a one-way valve to start pumping refrigerant vapor into the condenser.
2. Isobaric heating desorbs more refrigerant, forcing it into the condenser until state 3 is attained, at which the adsorber is nearly devoid of refrigerant.
3. The hot adsorber is then cooled isosterically (at constant total mass) causing adsorption and depressurization, until the pressure drops below P_e (state 4), opening another one-way valve to allow refrigerant vapor to enter the adsorber from the evaporator.
4. Isobaric cooling to state 1 saturates the adsorbent, completing the cycle.

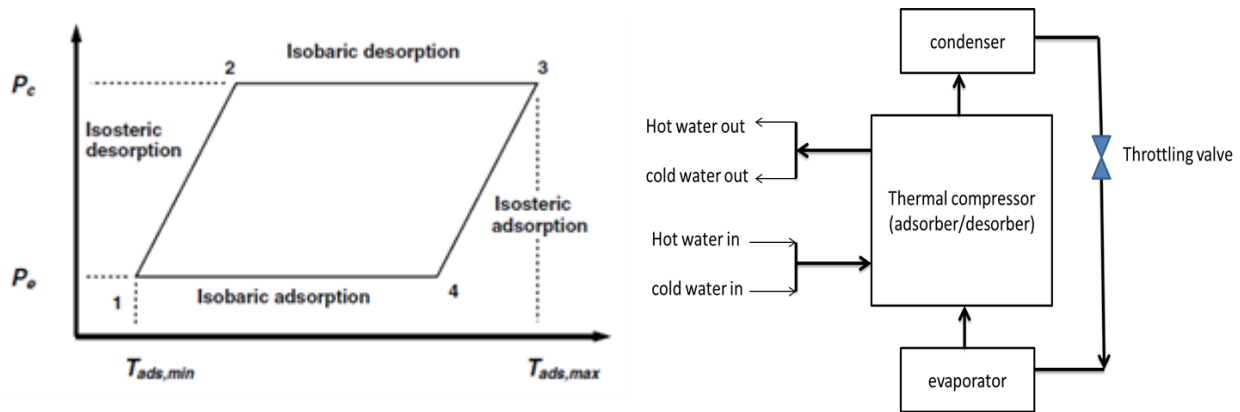


Figure 1. Thermodynamic cycle of the adsorption refrigeration, **Lambert, 2007**.

Wang, D., 2014, showed that the adsorption capacity of the silica gel was influenced by many factors. But pollution by solid particulates was the primary factor to decline the adsorption capacity.

Aristov, et al., 2012, investigated, using an intermittent cycle, the effect of the relative duration isobaric adsorption/desorption stages to maximize the coefficient of performance and the specific cooling power of the cycle. They found that the desorption phase is faster than the adsorption one and this should be considered as a routine case for adsorption refrigeration cycles, probably, because desorption occurs at higher temperature and pressure and hence, they suggested practical

Sapienza, et al., 2012, used a new composite sorbent to operate at low regeneration temperature ($< 70^{\circ}\text{C}$). Adsorption equilibrium measurements demonstrated that the new composite, LiNO_3 / Vermiculite exchange about 0.4 kg water/kg adsorbent in an exceptionally narrow temperature range, $33\text{-}36^{\circ}\text{C}$ (Adsorption at 12.6 mbar) and $62\text{-}65^{\circ}\text{C}$ (desorption at 56.2 mbar).

Gong et al., 2011, evaluated the composite material based on lithium chloride on silica gel as adsorbent and water as adsorbate in an adsorption chiller. The theoretical results showed that the COP can be increased using composite adsorbent.

Demir, et al., 2009, studied the effect of the granule size on the heat and mass transfer. The decrease of granule size enhances the contact area between the granules and consequently heat transfer rate through the bed; however it causes the increase of the mass transfer resistance.

Doau, et al., 2006, report results from an open cycle investigation aimed to determine the optimal salt content of CaCl_2 on the silica gel. The sorption equilibrium demonstrated that these materials can sorb 0.5-0.6 kg water/kg adsorbent at 12.3 mbar and 20°C .

In porous media, adsorption process is controlled by both adsorbate transportation and diffusion in adsorbent and inner reaction with adsorbent, between the two items, the transportation of gaseous adsorbate in the tunnel of micro pores and diffusion on its surface are more dominated than the internal reaction in rare pressure, **Wang, and Wang, 2005**.

Aristov, et al., 2002, studied the adsorption capacity of selective water sorbents by confining hygroscopic salt into the open pores of silica gel. The experimental results showed that the water uptake of CaCl_2 –in-silica gel was about 0.75 kg/kg at the temperature of 28°C while for silica gel is 0.1 kg/kg.

In this study, the attentions are focused on the mechanisms of mass transfer in the adsorbent bed of adsorption refrigeration system. The influences of temperature and cycle time on the adsorption velocity and adsorbate concentration rate are calculated. The governing equations for the mass transfer are presented and the solution method is described. The results are discussed via figures, which show the variations of temperature, adsorption velocity, and adsorption concentration in a circular bed. Finally, the practical cycle of the dynamic sorption is stated depicting all the operating conditions affected on the system.

2. ADSORPTION CAPACITY TEST

Brazilian commercial mesoporous and microporous silica gel was employed as the adsorbent for the adsorption chiller prototype **Table1.** water free from any ions was chosen as a refrigerant. For the heating/cooling system, water is the best heat transfer fluid (HTF), with the highest C_p of any liquid and higher thermal conductivity than all.

The silica gel was saturated whenever it was regenerated in an electric oven at 120°C for a minimum period of 24 h. After regenerating the silica gel, the adsorber was replaced immediately and was expected to cool down to room temperature, at which time and every one hour, it was weighed on a digital scale with a minimum accuracy of 5 g. The adsorptive adsorbers are coupled to the evaporator, which is a cylindrical container with a globe type valve used to control the passage of the adsorbate **Fig.1.** Before introducing water vapor from the evaporator into the adsorber, the vapor pipe from the evaporator toward the adsorber is evacuated to remove any traces of condensed water vapor, which cause experimental errors. The difference in weight of adsorber with silica gel before and after the adsorption interval period is the adsorbed water concentration.

Table. 1 Thermophysical properties of silica gel (values supplied by the manufacturer) .

Property	Value	Unit
Apparent density	750	Kg/m^3
Average particle diameter	7	mm
Specific surface area	650-700	m^2/g
Thermal conductivity	0.198	W/m.K
Specific heat capacity	921	J/kg.K

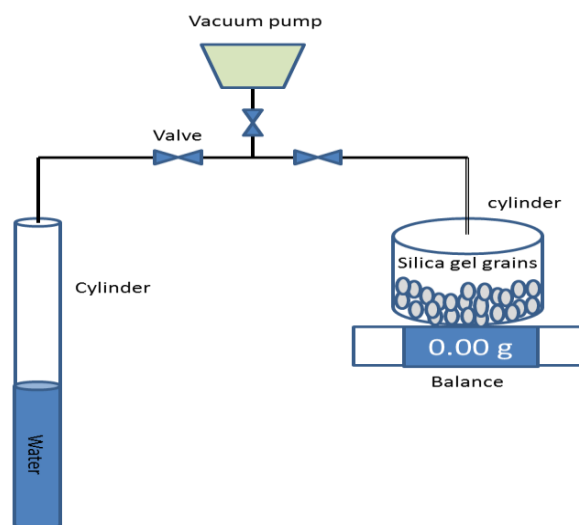


Figure 1. Equilibrium adsorption capacity apparatus.

3. DESCRIPTION AND PROCEDURE OF EXPERIMENTAL PROTOTYPE

Fig. 2 shows photographs of the experimental adsorption chiller prototype. The adsorption chiller has a single bed, a condenser, an evaporator and a heating/cooling water system. The evaporator lies at the bottom of the chiller and the condenser is located at the upper side. The heating system is next to the adsorber. All the valves are controlled manually. The prototype is designed to test various operating conditions and operating adsorption cycle. The whole prototype is connected to a water heating system for regeneration, tap water for cooling and adsorption, and a vacuum pump.

The main parameter was measured during the experiment: temperature variation with time. All sensors were connected to a data logger and recorded every 8.5 seconds. The data measurements were taken after the cycle steady state had been reached. A computer was used to collect and process the measurement data acquired by the data logger. The flow rate of hot water and cooling water are constant at 0.04 kg/s.

Fig. 3 illustrates the schematic diagram of the testing system. The adsorber is of the shell and fin-tube configuration which is readily (easily) manufactured, and it can withstand high operating pressure and incur low inert mass. The principle innovation of this design is that of internal heat exchanger of the adsorber. Using fins and tubes made the surface area to volume ratio relatively large. The fins on the adjacent four tubes overlap slightly in order to reach all portions of the shell void.

To complete one full cycle, the adsorbent bed passes through four consecutive steps: pre-heating, desorption, precooling, and adsorption. In the adsorber, about 4 kg silica gel is filled. The hot water temperature can be controlled in the range of 85–90°C. The flow rate of hot water is controlled by valve V7 and the cooling water is controlled by V8. V1 and V2 controlled the flow of the refrigerant from the adsorber to the condenser (desorption) and from the evaporator to the adsorber (adsorption), respectively. **Table. 2** reports the operating conditions of the tested adsorber where all the investigated tests conditions are displayed in terms of temperature and the duration of cycle time.



Figure 2. Pictorial of the experimental device.

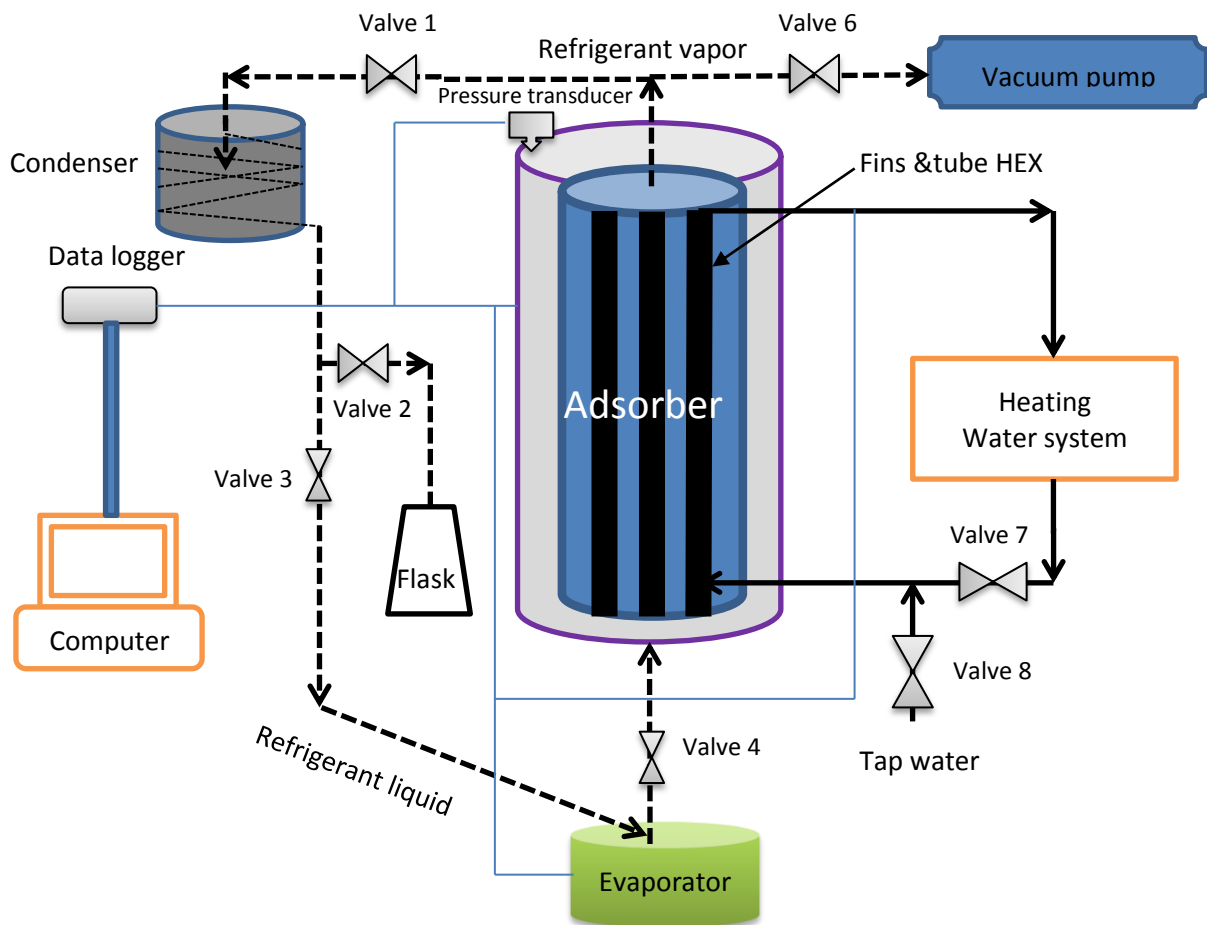


Figure 3. The schematic diagram of the experimental adsorption chiller.

Table 2. Experimental parameters for single bed silica gel-water prototype

Parameter	Value
T_e	11.2°C
T_c	30°C
T_{ads}	35°C
T_{des}	90°C
$t_{iso-heating}$	1.25 min
$t_{iso-cooling}$	1.25 min
t_{des}	18.75 min
t_{ads}	18.75 min
t_{cyc}	40 min

4. NON-EQUILIBRIUM ADSORPTION MODEL

For refrigeration applications, the adsorbent should have high adsorptive capacity at ambient temperature and low pressure, and small capacity of adsorption at high temperature and pressure, **Leite, et al., 2004**. Two types of mass transfer are encountered in a granular adsorbent bed : mass transfer within the adsorbent granules and mass transfer through the void between the granules (i.e intra-particulate and inter-particle mass transfer) , **Demir et al., 2009**. The equilibrium adsorption quantity is the amount of refrigerant adsorbed by the sorbent when the reaction time tends towards infinite, and it is an important parameter for adsorption working pairs. In general, the velocity of adsorption in adsorber is not faster than that of heat transfer, that is, the desorption rate does not reach the equilibrium value at each status point in real operation, **Wang, and Wang, 2005**. Moreover, the actual process of adsorption/desorption is of non-equilibrium and it actually relies on the mass transport process. Therefore, actual adsorption process is not the process only dominated by the temperature of adsorbent and pressure of the adsorbate, it is involved with mass transport and diffusion, **Wang, and Wang, 2005**.

The equilibrium model for this physical adsorption concentration (x^*) is a function of adsorbent temperature and pressure, and it is written in a generic form as, **Liu, et al., 2005**.

$$x^* = f(T, P)$$

Models with different fixed parameters are as follows:

$$x^* = f(P)_T \text{ Isothermal}$$

$$x^* = f(T)_P \text{ Isobaric}$$

$$P = f(T)_x \text{ Isosteric}$$

These functions correlate the temperature T , the pressure P and the concentration of the adsorbed phase x , so that $f(T, P, x) = 0$. For equilibrium of adsorption in microporous materials with a polymodal distribution of pore dimensions, such as the silica gel-water and activated carbon-methanol pair, Dubinin and Astakhov proposed the following isotherms, **Dieng, and Wang, 2001**.

$$x^* = x_o \exp \left[-K \left(RT_b * \ln \left(\frac{P_b}{P_{c/e}} \right) \right)^n \right] \quad (1)$$

Where:

$$P_c (T_c = 30^\circ C) = 4.42 \text{ Kpa}$$

$$P_e (T_e = 7^\circ C) = 1 \text{ Kpa}$$

Sakoda and Suzuki, (1984) considered the influence of diffusion on the micropores surface, proposed the model of adsorption velocity as below (2). When the analysis is simplified, the lagging effect between adsorption and desorption is neglected:

$$\frac{dx}{dt} = k_m (x^* - x) \quad (2)$$

$$x(t) = x^* \cdot (1 - e^{-k_m \cdot t}) \quad (3)$$

$$k_m = \left(\frac{15D_o}{R_p^2} \right) \exp \left(\frac{-E_a}{RT_b} \right) \quad (4)$$

The saturation vapor pressure and temperature are correlated by Antonio's equation which can be written as ,**Khan, et al., 2006.**

$$P_b = 133.32 * \left(\exp \left(18.3 - \frac{3820}{T_b + 273 - 46.1} \right) \right) \quad (5)$$

Firstly, the equilibrium adsorbate concentration within the adsorbent granule is evaluated by using Eq. (1) at the specified temperature and pressure Eq. 5. Eq. (4) is solved to find the adsorption rate constant. Based on all these calculations, Eq. (3) and Eq. (4) are solved to find the adsorption velocity and the simultaneous concentration distribution. An iteration is performed before increasing a time step. The iteration is continued until the time of the phase is completed.

5. RESULTS AND DISSCUTION

The adsorption isotherm of water on silica gel (Brazilian type) is presented in **Fig. 4.**The experimental results include equilibrium water uptake when the silica gel was exposed to saturated water vapor at operating temperature, 30°C. It is shown that the maximum equilibrium adsorption capacity is 0.2 kg water \ kg adsorbent.

Fig. 5 shows the temporal evolution of the isosteric cooling, isosteric heating, desorption and adsorption cycles at a steady state for the following operating conditions concluded from the experiment test.

The adsorption rate constant decreased when temperature was lowered, which means that the adsorption was taking longer time at lower temperatures, **Fig. 6.**

Fig. 7 shows the time change in the amount of adsorbed water vapor measured at various regeneration temperatures. As seen in this figure, the amount of adsorbed water increases with

time for the same temperature, but decreases with regeneration temperatures. However, effective adsorptivity did not reach the value equal to maximum state recorded from experimental results of water adsorption isotherm of silica gel, χ^* ; e.g. at 30°C, χ^* is 0.13 kg/kg for 20 min, whereas χ^* is 0.2 kg/kg. Using these results, it was determined that 35 % of silica gel was not effectively used in cycle operation.

The experimental values of the adsorption velocity (dx/dt) as a function of adsorption time using a single adsorber bed are reported in **Fig. 8**. The operating conditions selected are the following: $T_c = 30^\circ\text{C}$, $T_{ads} = 35^\circ\text{C}$, and $T_{des} = 90^\circ\text{C}$. Results obtained demonstrated that the adsorption velocity was diminished after 20 mins. There is a very low value of adsorption velocity after 20 mins, and it may not be enough to keep the temperature of the water inside the evaporator at the designed value.

Desorption process is very close in concentration change to adsorption process, and many researches assume both are the same in adsorption refrigeration process. It is clear from experimental results that after 20 mins, the concentration of water into silica gel reaches 0.048 kg water/kg adsorbent **Fig. 9**. It is very close to the calculated value, 0.04 kg/kg, by using Eq. (3)

Fig 10.

Based on this non-equilibrium model Eq.(3), some calculations using experimental results have been done to discover the effect of non-equilibrium adsorption on adsorption refrigeration **Fig. 10**. It could be observed that the non-equilibrium deviates from the equilibrium particularly for a time shorter than 40 min., and for the first time, this deviation does not seem very big. For example, the value of non-equilibrium adsorption rate at 20 min. is 0.12 kg/kg while for the equilibrium rate; it is 0.124 kg/kg. This difference of 0.004 kg water/kg adsorbent can produce a cooling power of 9.908 kJ/kg adsorbent. Without doubt, the non-equilibrium model is closer to the real process of adsorption refrigeration and should not be neglected on designing cycle adsorption chiller, especially when the cycle is short because in real short cycle, the adsorbed refrigerant could not be sufficient due to the non-equilibrium adsorption process, **Wang and Wang, 2005**. In the same figure **Fig. 10**, the non-equilibrium desorption process is very close to the equilibrium and the reason is simply because of the high rate constant of the desorption process.

Fig. 11 aims to determine the dynamic water sorption, which represents the amount of water involved in one adsorption-desorption cycle. The experiment has consisted of loading adsorbent with water under a temperature of 35°C, then the adsorbent were, afterwards, desorbed at the temperature of 90°C in the same duration as the adsorption time. The difference between adsorbent loading at the end of the adsorption, $\chi = 0.12$ kg/kg, and its loading at the end of desorption, $\chi = 0.04$ kg/kg, constitutes the dynamic water sorption. The measurement of the adsorption capacity of this type of silica-gel showed that it is able to exchange a large amount of water of 0.08 kg/kg under operating conditions so it is typical for air conditioning applications as well as to be driven by hot water temperature of 90°C.

A complete cycle of adsorption/desorption for the silica gel-water adsorber is shown in **Fig. 12**. During the adsorption phase, the maximum value reached is 0.12 kg/kg after the first half-cycle of 20 mins, and the minimum is 0.04 kg/kg during the second half-cycle of 20 mins. this value is perhaps the target to get the best performance of the system.

To demonstrate the practical cycle of adsorption chiller using a silica gel-water system, **Fig 13** presents the calculated data using Eqs. (1-5) at two worked isobar pressure ranges, namely the vapor pressure of evaporator ($T_e = 7^\circ\text{C}$, $P_e = 1$ kpa), A-D curve, and the condenser ($T_c = 30^\circ\text{C}$, $P_c = 4.2$ kpa), B-C curve, where A-B and C-D lines represent isotherming cooling and heating phases respectively. Measuring isobars of water adsorption/desorption is useful for drawing a temporary cycle of the adsorptive chiller and determining the boundary temperatures for the adsorption and desorption processes. Isobars of water adsorption at $P = 1$ kpa and desorption at $P = 4.2$ kpa

measured for the sorption of silica gel-water represent the isobaric stages of a typical chiller cycle **Fig. 6.12**. The highest desorption temperature was fixed at 90°C, that determined the content of the water, with $x = 0.04$ kg/kg. Desorption of water started at 60.5°C, and finished at 90°C (isobar line B-C). The lowest adsorption temperature of 35°C resulted in the maximal adsorbed amount of $x = 0.124$ kg/kg. Adsorption of water started at 62°C, and finished at 35°C (isobar line D-A). This shows the properties of this type of silica gel to exchange 0.084 kg/kg is very close to the experimental result obtained by the practical test work **Fig. 11**. As mentioned above, **Fig. 13** will help us to assess the level of temperatures of alternating adsorption to desorption and vice versa, but it is still not able to compare it with the experimental cycle because there is no instrument that can measure the change of water concentration into silica gel with the temperature directly.

5. CONCLUSIONS

The mass transfer in a cylindrical annulus bed packed with silica gel granules during the adsorption/desorption process were analyzed. The measurement of adsorption rates using a non-equilibrium model shows that this type of silica gel is able to exchange an amount of 0.08 kg water/kg adsorbent under the operating conditions of 90°C desorption temperature, 35°C adsorption temperature, and cycle time of 40 min. the practical cycle indicated that the system has the ability to work under different operating system due to its dynamic sorption variation. Thus, this type of adsorbent should be a good candidate for various thermal applications driven by low temperature heat sources.

REFERENCES

- Aristov Y.I., Sapienza A., Ovoshchnikov D.S., Freni A., and Restuccia G., 2012. *Reallocation of Adsorption and Desorption Times for Optimisation of Cooling Cycles*. Internal journal of refrigeration, Vol. 35, PP. 525-531.
- Aristov Y.I., Restuccia G., and Parmon V.N., 2002, *A Family of New Working Materials for Solid Sorption Air Conditioning Systems*, Applied thermal engineering, Vol. 22, PP.191-204.
- Dao K., Wang R.Z., and Xia Z.Z., 2006, *Development of a New Synthesized Adsorbent for Refrigeration and Air Conditioning Applications*, Applied Thermal Engineering, Vol. 26, PP. 56-65.
- Demir H., Mobedi M., and Ulku S., 2009, *Effect of Porosity on Heat and Mass Transfer in a Granular Adsorbent Bed*, International communications in Heat and Mass Transfer, Vol. 36, PP. 372–377.
- Dieng A.O., and Wang R.Z., 2001, *Literature Review on Solar Adsorption Technologies for Ice-Making and Air Conditioning Purposes and Recent Developments in Solar Technology*. Renewable and Sustainable Energy Reviews, Vol. 5, PP. 313–342.
- Gong L.X., Wang R.Z., Xia Z.Z., Chen C.J., 2011, *Design and Performance Prediction of a New Generation Adsorption Chiller Using Composite Adsorbent*, Energy Convers Manage, Vol. 52, PP. 2345-50.
- Khan M.Z.I., Alam K.C.A., Saha B.B., Hamamoto Y., Akisawa A., and Kashiwagi T., (2006), *Parametric study of a Two-Stage adsorption Chiller using Re-Heat-the Effect of Overall*



Thermal Conductance and Adsorbent Mass on System Performance. International Journal of Thermal science, Vol. 45, PP. 511-519.

- Lambert M. A., 2007, *Design of Solar Powered Adsorption Heat Pump with Ice Storage*, Applied Thermal Engineering, Vol. 27, PP. 1612–1628.
- Leite A.P., Grilo M.B., Belo F.A., and Andrade P.R., 2004, *Dimensioning, Thermal Analysis and Experimental Heat Loss Coefficients of An Adsorbitive Solar Ice maker*, Renewable Energy, Vol. 29, PP. 1643-1663.
- Liu Y.L., Wang R.Z. and Xia Z.Z., 2005. *Experimental Performance of a Silica Gel–Water Adsorption Chiller*. Applied Thermal Engineering, Vol. 25, PP. 359–375.
- Sapienzaa A.I., Glaznevb I.S., Santamariaa S.A., Frenia A.N., and Aristov Y.I., 2012, *Adsorption Chilling Driven by Low Temperature Heat: New Adsorbent and Cycle Optimization*, Applied Thermal Engineering, Vol. 32, PP.141-146.
- Wang D., Zhang J., Yang Q., Li N., and Sumathy K., 2014, *Study of Adsorption Characteristics in Silica Gel–Water Adsorption Refrigeration*, Applied Energy, Vol.113, PP.734–741.
- Wang, W. and Wang, R., 2005, *Investigation of Non-Equilibrium Adsorption Character in Solid Adsorption Refrigeration Cycle*, Heat Mass Transfer, Vol. 41, PP. 680-684.

NOMENCULATUR

$b =$	bed
$D_o =$	surface reference diffusivity constant, $2,5 \cdot 10^{-4} \text{ m}^2/\text{s}$
$E_a =$	diffusion activation energy, $2.33 \cdot 10^6 \text{ J/kg}$
HTF =	heat transfer fluid
$K =$	coefficients of the D–A equation = 0.004912 kg/J
$k_m =$	adsorption rate constant, m^2/s
$n =$	linear driving force relation constant (for the Brazilian silica gel = 1)
$P_c =$	condensing pressure, kpa
$P_e =$	evaporating pressure, kpa
$R =$	ideal gas constant, 0.462 J/kg.K
$R_p =$	radius of adsorbent particle, m
$T_{ads} =$	adsorption Temperature, °C
$T_{des} =$	desorption temperature, °C
$T_c =$	condensing temperature, °C
$T_e =$	evaporating temperature, °C
$T_{iso-cooling} =$	isosteraing cooling temperature, °C
$T_{iso-heating} =$	isosteraing heating temperature, °C
$t_{cycle} =$	cycle Time, min
$x =$	adsorbate concentration, kg water/kg adsorbent
$x_o =$	maximum adsorption capacity, kg water/kg adsorbent
$x^* =$	equilibrium adsorption capacity, kg water/kg adsorbent
$\Delta x =$	difference of adsorbate content, kg water/kg adsorbent

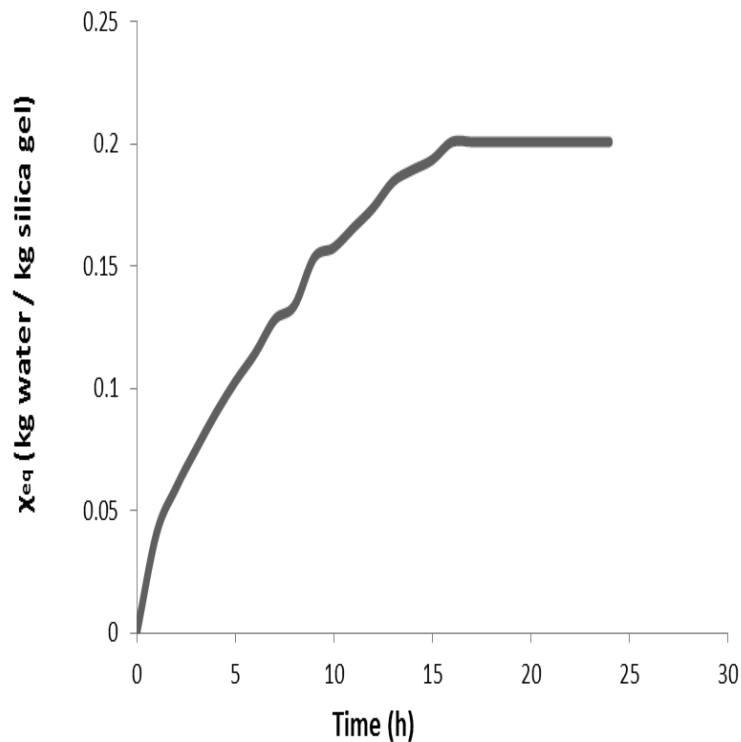


Figure 4. Equilibrium water uptake on silica gel adsorbents at 30°C.

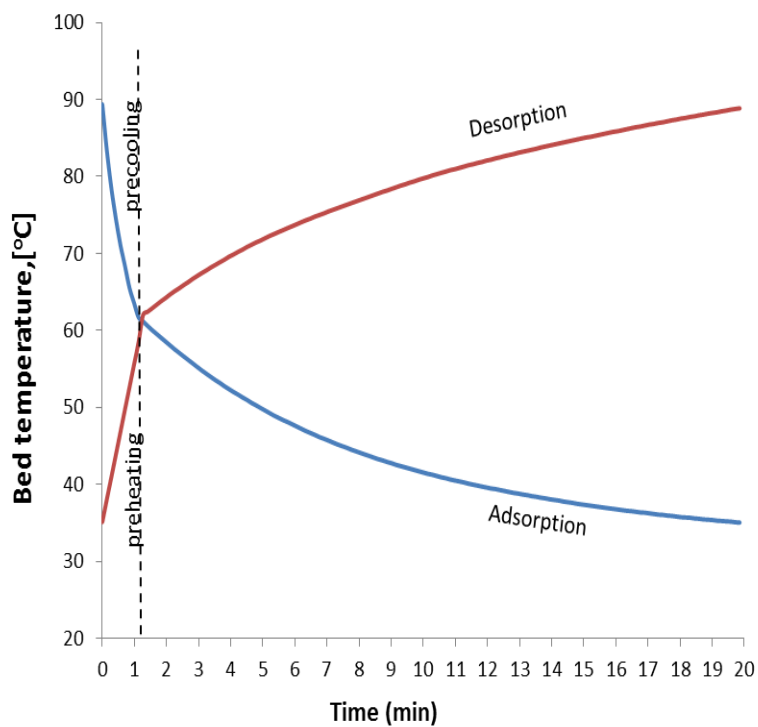


Figure 5. Preheating+ desorption/ precooling + adsorption temporal variation with time.

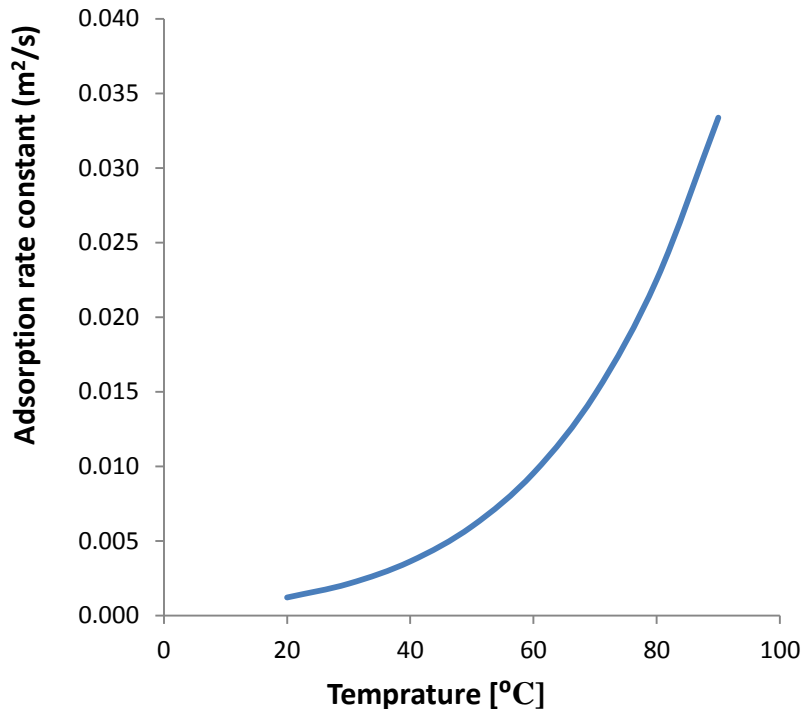


Figure 6. Adsorption rate constant variation with temperature.

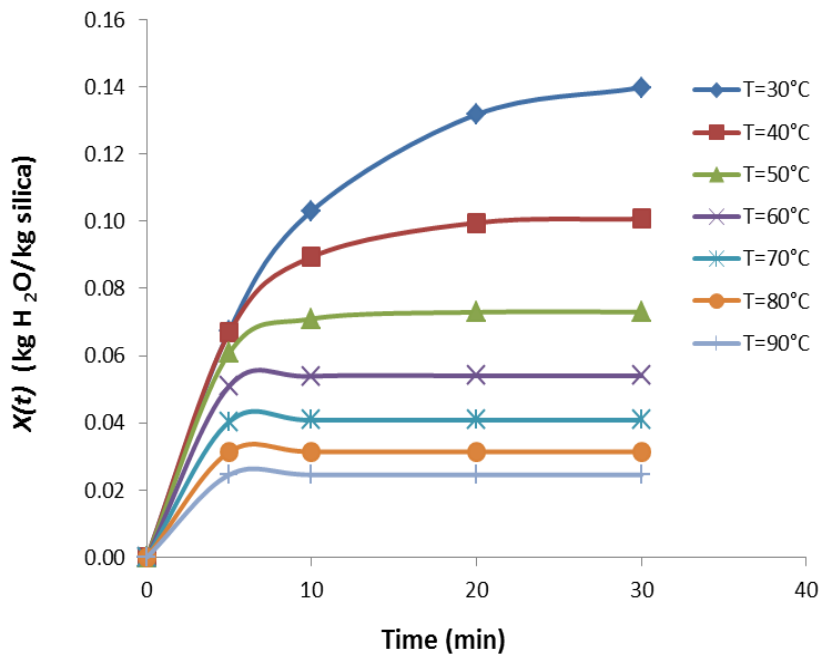


Figure 7. Adsorption uptake variation with time at constant temperature.

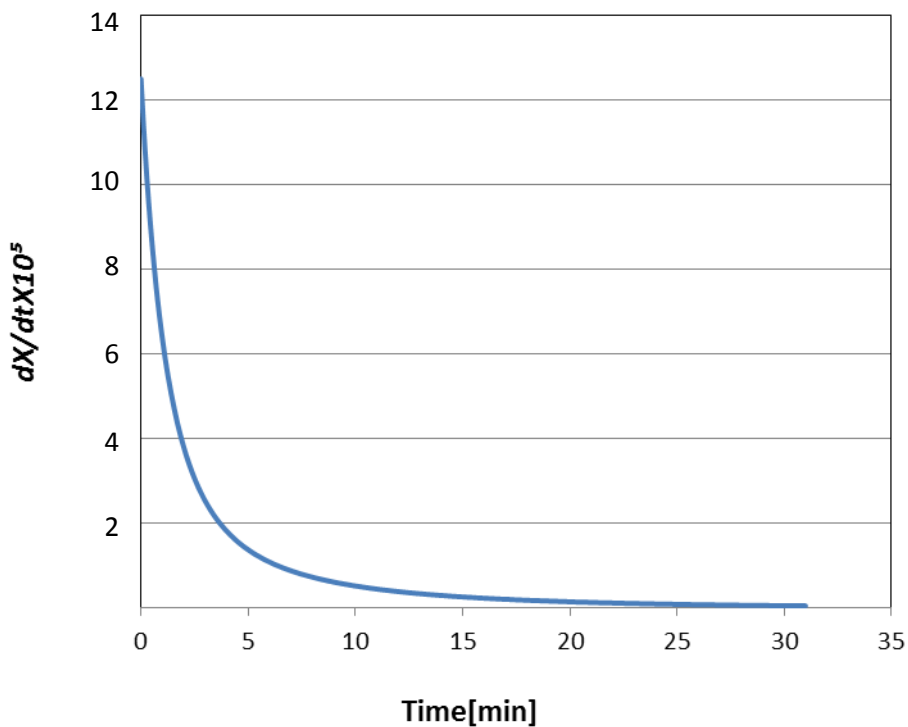


Figure 8. Adsorption velocity variation with time ($T_c = 30^\circ\text{C}$, $T_{ads} = 35^\circ\text{C}$, $T_{des} = 90^\circ\text{C}$).

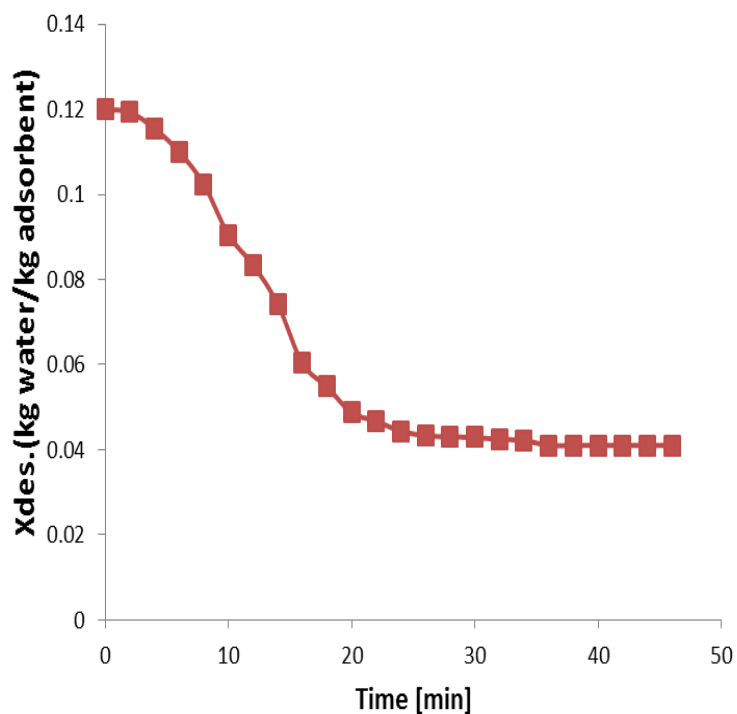


Figure 9. Experimental desorption results variation with time at 90°C hot water.

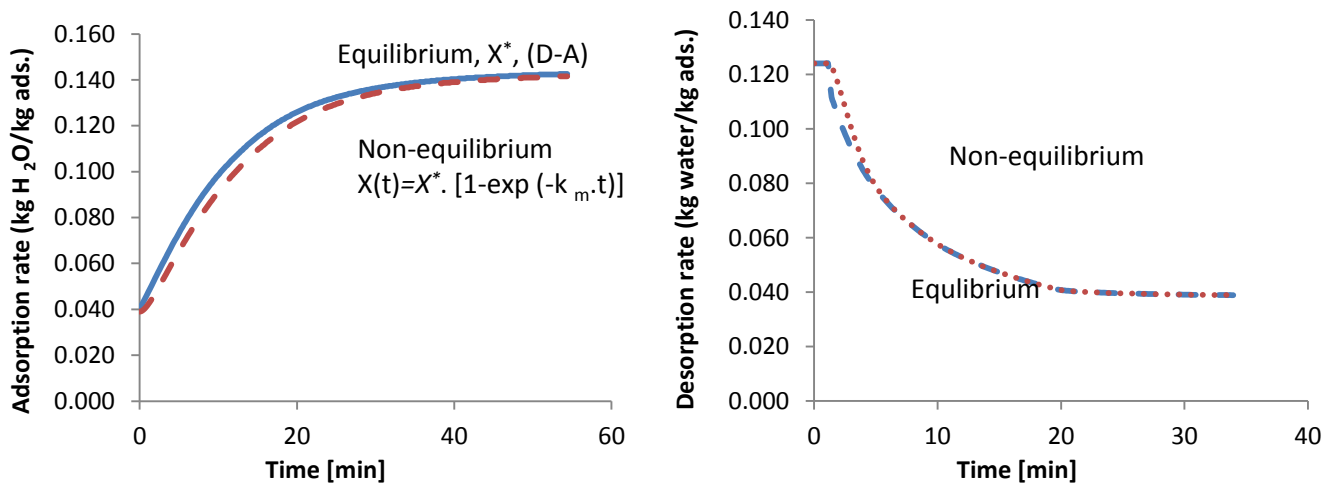


Figure 10. Comparison between equilibrium and non-equilibrium models.

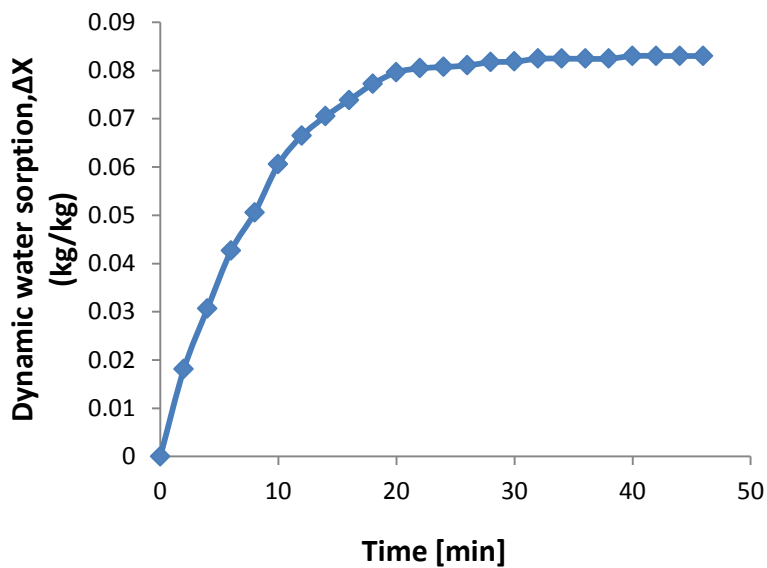


Figure 11. Dynamic water sorption.

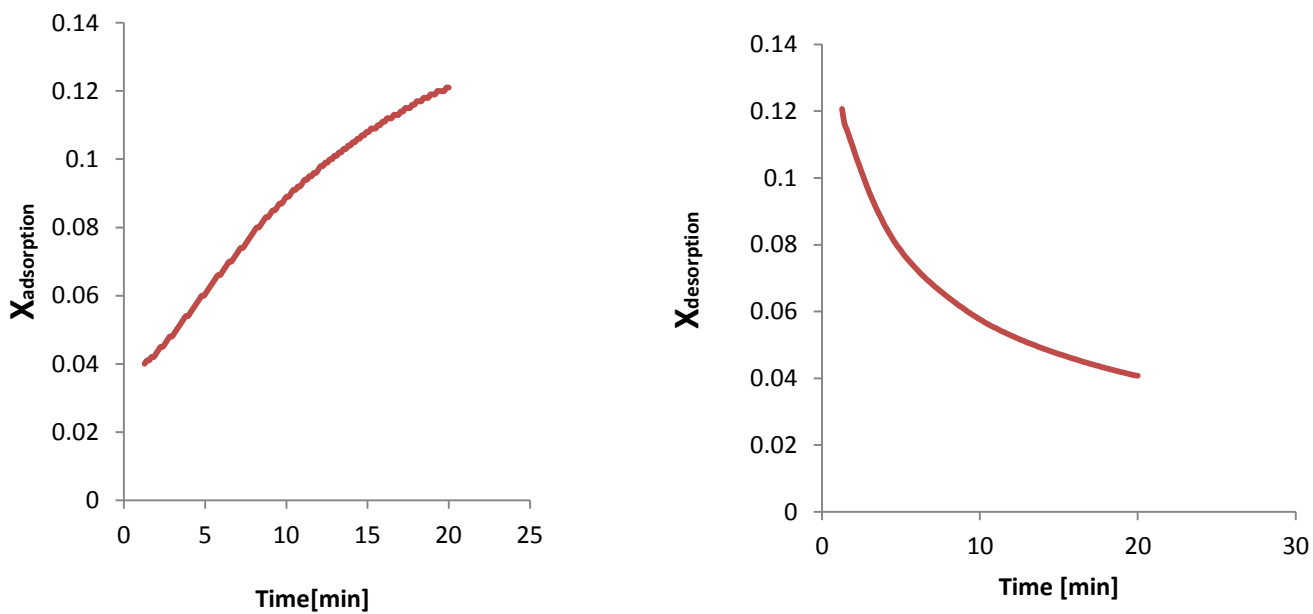


Figure 12. Adsorption/Desorption rate variation with time.

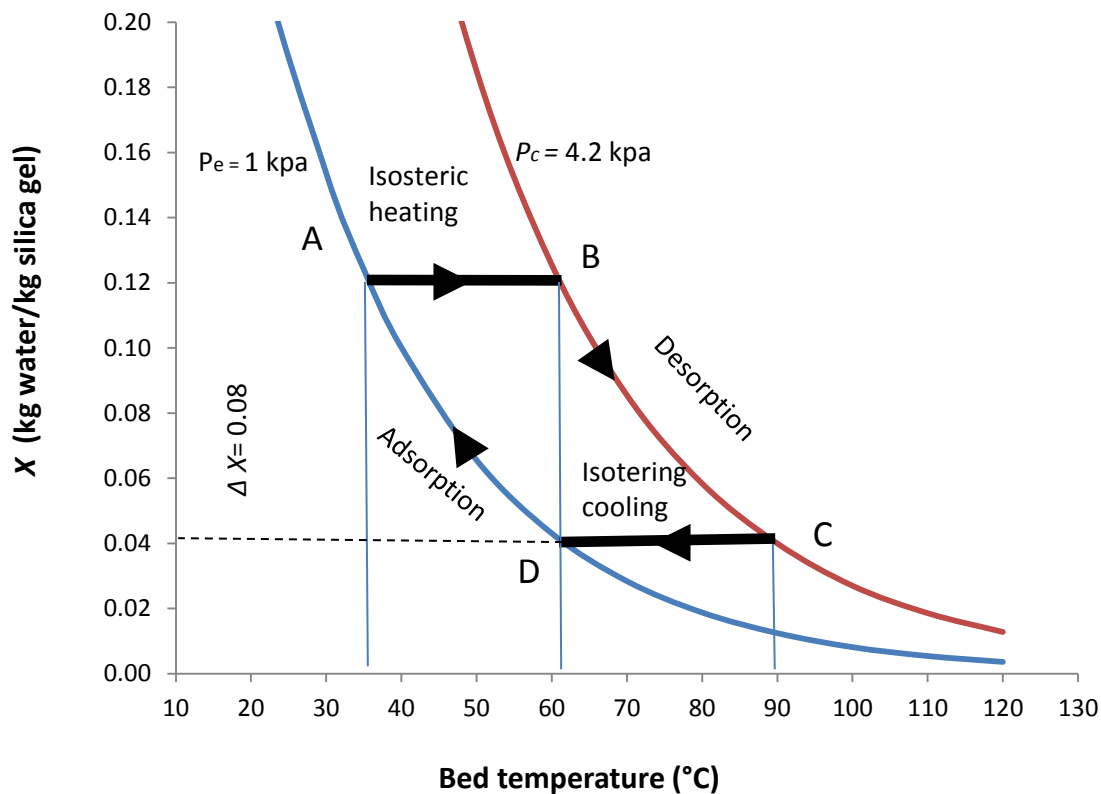


Figure 13. Practical cycles of adsorption and desorption ($T_{des}=90^\circ\text{C}$, $T_{ads}=35^\circ\text{C}$).